Physica Scripta

ACCEPTED MANUSCRIPT

Temperature measurement using a microfiber knot ring encapsulated in PDMS

To cite this article before publication: Rui Fan *et al* 2019 *Phys. Scr.* in press https://doi.org/10.1088/1402-4896/ab34ec

Temperature Measurement Using a Microfiber Knot Ring Encapsulated in PDMS

Rui Fan[1], Juntong Yang[1], and Jin Li[1, 2]* and Fanli meng[1]

[1]*College of Information Science and Engineering, Northeastern University, Shenyang, 110819, China*

[2]*State Key Laboratory of Applied Optics, Changchun Institute of Optics, Fine Mechanics and Physics, Chinese Academy of Sciences, Changchun 130033,China*

***E-mail:** lijin@ise.neu.edu.cn

Abstract: A microfiber knot ring (MKR) with a temperature sensitivity of 183 pm/°C has been proposed and experimentally demonstrated. To further improve its stability and sensitivity, the polydimethylsiloxane (PDMS) film was used to encapsulate it to be a slice probe. The temperature sensitivity was increased for more than 9 folds with a good stability and repeatability. The contribution ratios of thermal-optic coefficient and thermal-expansion coefficient of silica and PDMS were analyzed and discussed. The high sensitivity of 1.67 nm/°C and miniature slice structure enables its application for precisely monitoring the temperature fluctuation in some special occasions.

Keywords: Microfiber; Fiber sensor; Temperature sensor; Microfiber knot ring (MKR); Polydimethylsiloxane (PDMS).

Introduction

Accurate temperature monitoring is critical important in many occasions, such as the industrial processes controlling, photovoltaic devices efficiency, health monitoring, biological molecular activities and chemical reactions adjustment [1-3]. In recent years, optical fiber temperature sensor has attracted much attention because of its unique advantages compared with electrical sensor, such as the anti-electromagnetic interference, small size, high sensitivity and good flexibility [4-7]. It can be concluded from the reported works that these temperature fiber sensors were usually constructed by different kinds of special fibers or microstructures [8] relying on complex micro/nano-processing fabrication schedules [9] or expensive equipment [10]. For example, the multicore fiber or laser written fiber Bragg fiber can operate at high temperature of 1000 ℃ to measure the temperature change with the sensitivity of dozens of pm/°C in a wide working range [11, 12]. The high sensitivity and wide working range are always mutually restrictive depending on their applications. In contrast, the low-cost single-mode fiber will be the most promising candidate to reduce cost and simplify process for exploring the commercial temperature sensors. Various related forms and structures have been reported and covered the fiber ring resonators, fiber interferometers and microfiber tapers [13-16]. Based on the high efficiency coupling of the evanescent wave between optical micro/nano-scale waveguides, the microfiber knot resonator (MKR) has been designed and fabricated to realize sensing devices with the high sensitivity, stable structure and flexible morphological parameters [17-19]. The sensing performance of MKR structure constructed by a single material is easier to study because the corresponding morphology parameters can be controlled precisely, but its long-term stability and sensitivity will be limited by the fiber material. For example, the sensitivity of silica MKR and poly(methylmethacrylate) (PMMA) MKR temperature sensor are dozens of pm/°C and 0.266 nm/°C, respectively [20, 21]. Many function materials have been introduced into the MKR to obtain a more excellent sensing performance [22-24]. Where, the graphene film has been demonstrated to reduce the response time to as fast as 56 ms due to the high electrons transfer rate [25]; the polytetrafluoroethylene (PTFE) with excellent corrosion resistance, high temperature

resistance and low friction coefficient was used to improve its stability [26]; the micrometers thickness of polydimethylsiloxane (PDMS) film was theoretically demonstrated to improve the sensitivity of MKR temperature sensor to be up to 0.197 nm/°C [27].

In this paper, the MKR structures were prepared by the microfiber with the diameter of several micrometers, which was obtained from common single mode fiber using the one step flame heating-drawing technique. The temperature sensing performance of both bare MKR and PDMS packaged MKR has been experimentally demonstrated and compared.

Experimental Methods

The experiment schematic was illustrated in Fig. 1(a), the amplified spontaneous emission (ASE-C source, 1520-1580 nm) was used as the light source.

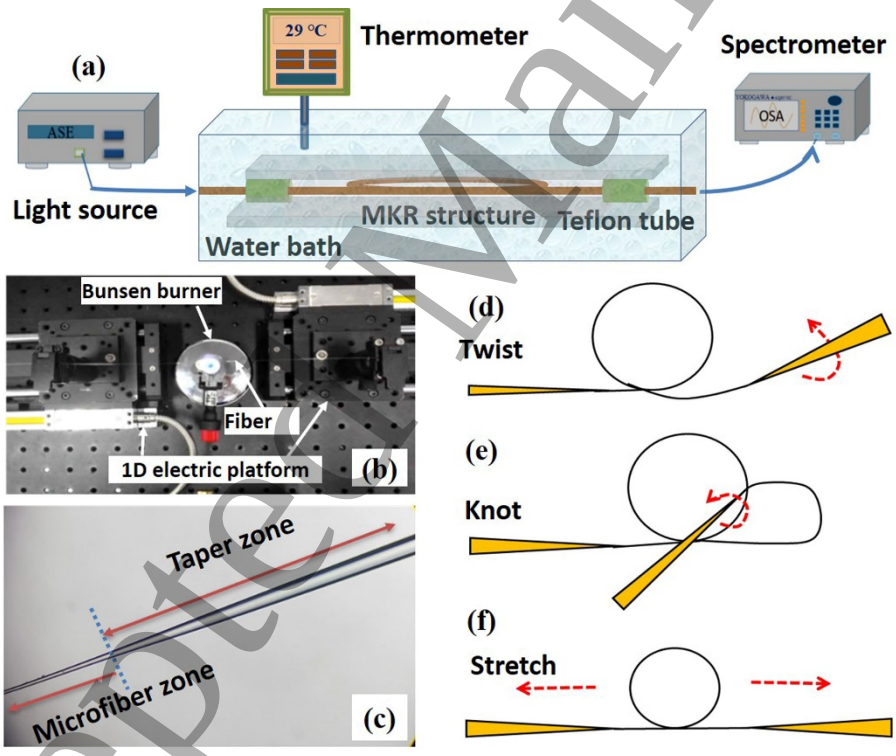

Fig. 1. (a) Schematic diagram of temperature sensing experiment for MKR structure; (b) Microfiber preparation system based on flame-heating and self-modulation stretching technique; (c) Photo of microfiber taper; Fabrication process of microfiber knot resonator using three-steps method, including (d) circling, (e) knotting and (f) stretching.

The MKR structure was sandwiched by two glass slides and encapsulated by PDMS, whose thickness was controlled by two Teflon tubes. The whole temperature probe was

immersed in the water bath environment and the corresponding temperature values were monitored by a thermometer (EBRO FXT430). The transmission spectra were collected and analyzed by the optical spectra analyzer (OSA, YOKOGAWA AQ6370) with the resolution of 20 pm. To obtain the microfiber, we built a homemade flame heating-drawing system, as shown in Fig. 1(b), including a Bunsen burner (Dragon-200, highest temperature 1300 ℃) and two one dimensional electric displacement platforms being equipped with two fiber holders. The diameter of the microfiber can be manipulated by changing the drawing speed, flame temperature and heating region. It can be seen from Fig. 1(c) that the microfiber has the smooth surface and the uniform conical region. The MKR structure was fabricated following the schedules in Fig. 1(d-f), where one end of microfiber was inserted through the ring, and then both two ends of microfiber were stretched in the opposite directions. The ring diameter was seriously limited by the microfiber diameter, as too small ring will be fragile and result in the serious leakage of light signals. Smaller diameter of microfiber can support the stronger evanescent wave to get a smaller ring resonator without serious light loss.

Experimental Results and Analysis

The temperature sensing performance of a bare MKR structure with the microfiber diameter of ~8.6 μm and the ring diameter of ~4.5 mm was determined in the temperature range of 20-70 ℃. The transmission spectra were recorded with a step of 10 ℃, where two resonance dips were obtained and red-shifted continuously with a value of ~9.15 nm due to the thermal-optical effect of silica [28]. As muti-dips turn out in the spectra, the whole temperature range of 50 ℃ was used in the experiment to make sure that the resonances dip shifts in one free spectra range. In this case, the different dips won not overlap with each other and can be distinguished.

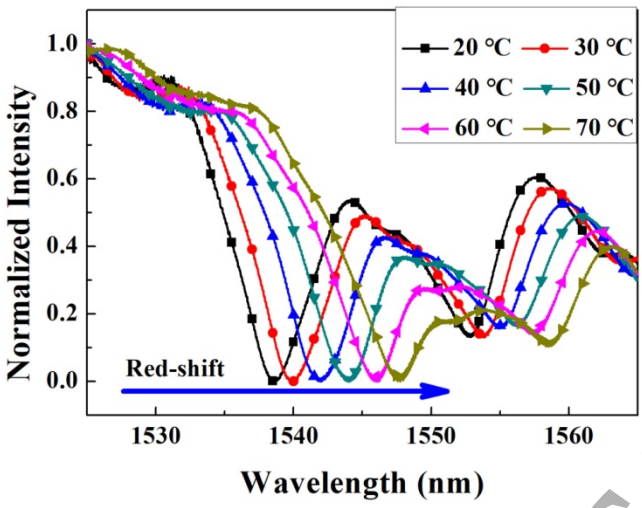

Fig. 2. Transmission spectra of bare MKR structure for temperature increasing from 20 °C to 70 °C with a step of 10 °C.

The same MKR was later packaged in the PDMS film. Where, the basic component and curing agent (with the weight ratio of 10:1) was being stirred for 5 min to get the PDMS sol, which was stewed for 4 hours to eliminate the air bubbles. MKR structure was placed on a piece of glass slide and covered with PDMS sol. Another glass slide was covered to package the MKR as a sandwiched structure. Two Teflon tubes with the diameter of 0.6 mm were inserted between the two slides to promise the fixed thickness of the PDMS film. The packaged probe was cured in a thermostat for 1 hour at 100 °C. The cured PDMS film acts the thermal sensitive material with the thermal-expansion coefficient of 3.0×10^{-4} /°C [29] and the thermal-optical coefficient of -100×10^{-6} RIU/°C [30], which are higher than those of silica. Furthermore, either the structure expansion or refractive index decrease will contribute to the blue shift of resonant dips, as demonstrated experimentally in Fig. 3(a).

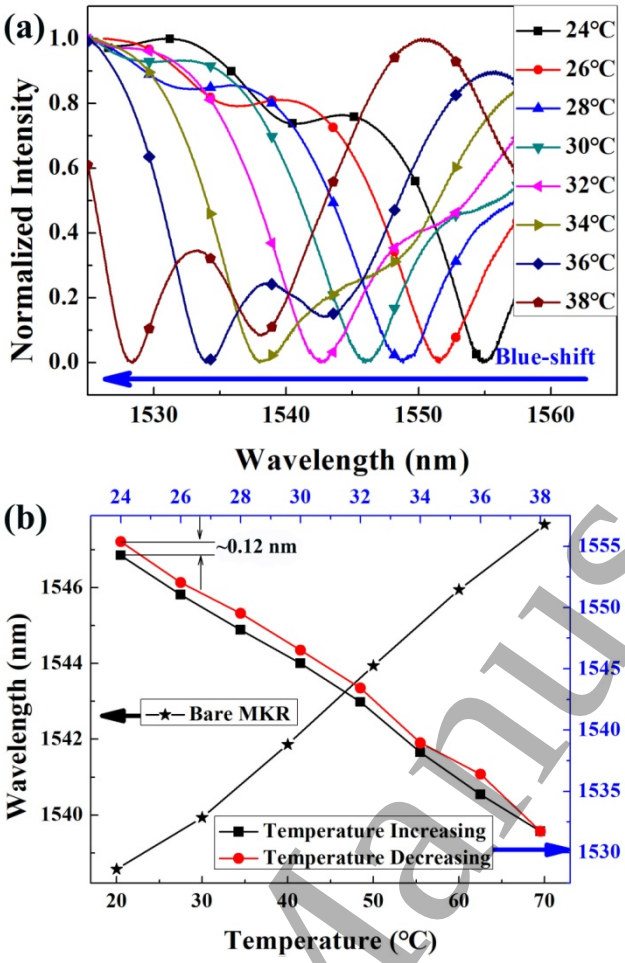

Fig. 3. (a) Transmission spectra of PDMS packaged MKR structure for temperature increasing from 24 °C to 38 °C with a blue-shifted resonance dip. (b) Temperature sensing performance comparison between bare MKR (increasing from 20 °C→70 °C) and PDMS-MKR (round trip during 24 °C↔ 38 °C).

When the temperature increased from 24 °C to 38 °C with a step of 2 °C, the resonance dip blue-shifted for ~23.37 nm with the average sensitivity of 1.67 nm/°C. The temperature range was limited by the big shift of resonance dip. After the temperature increasing for 14 °C, the resonance dip has shifted for more than 20 nm. Furthermore, two resonance dips turned out in the spectra and difficult to distinguish, which will limit the working range of the temperature sensor. So the proposed temperature sensor probe only can operate in a limited working range to monitor the temperature fluctuation with ultra high sensitivity or resolution. To explore the temperature sensing performance in other intervals, one can trace the resonance dip during the special temperature range. For the proposed temperature sensor, its maximum working range will be limited by PDMS. When the temperature decreased from 38 °C to 24 °C with a step of 2 °C, the resonance dip red-shifted backward to the

initial location with a deviation of ~0.12 nm, as indicated in Fig. 3(b). Furthermore, the resonance dip slowly moved back to its previous wavelength at the fixed temperature value of 24 ℃, the deviation value reduced to be lower than the resolution of OSA. The possible reason can be attributed to the different thermal response time of PDMS during the temperature increasing and decreasing process, where the expansion rate is faster than that of shrink.

To verify the thermal response time of the PDMS-MKR temperature sensor, the locations of the resonance dip was continuously recorded for every 5 s when the temperature probe was immersed alternately in the two thermostat water baths with the temperature of 32 ℃ and 28 ℃, respectively. For a fixed temperature environment, the resonance dip was stable and no significant shift was observed in the experimental results, as shown in Fig. 4.

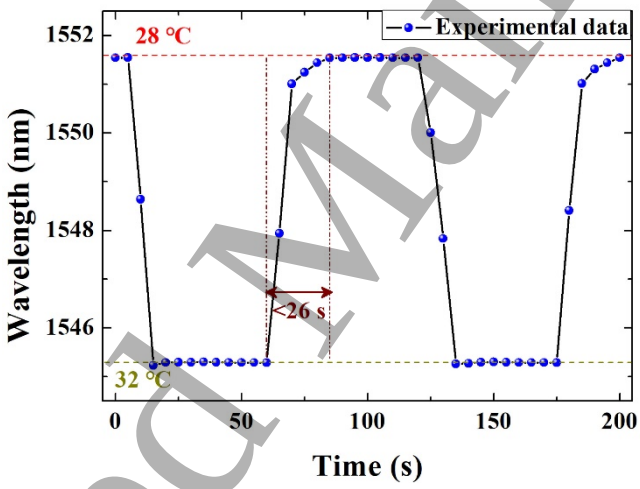

Fig. 4. Temperature response of PDMS-MKR structure for temperature changing between 28 ℃ and 32 ℃.

When the temperature was changed from 32 ℃ to 28 ℃, the resonance dip red-shifted quickly and then slowly moved to a fix location in less than 26 s. Furthermore, it can be determined from the experiment curve that the response time was less than 15 s for the temperature increasing process. These experimental results met well with the thermal expansion property of PDMS the analyzed in the former section.

In this work, on one hand, the PDMS film was introduced to improve the temperature sensitivity of silica MKR structure, as mentioned and discussed above; on the other

hand, the PDMS film can protect the fragile MKR to improve its stability and prolong its service life. The high temperature sensitivity depends on the high thermal-expansion coefficient and the negative thermal-optical coefficient of PDMS film. Assuming their contributions are a_E and a_O, respectively. The temperature sensitivity of the PDMS-MKR and the bare MKR are:

$$S_{PDMS-MKR} = \begin{pmatrix} a_E \\ a_O \end{pmatrix} \begin{pmatrix} E_{PDMS} & O_{PDMS} \\ E_{Silica} & O_{Silica} \end{pmatrix} \quad (1)$$

$$S_{MKR} = \begin{pmatrix} a_E \\ a_O \end{pmatrix} \begin{pmatrix} E_{Silica} & O_{Silica} \end{pmatrix} \quad (2)$$

By substituting sensitivity values of both PDMS-MKR and bare MKR, as well as the characteristic parameters of PDMS and silica into the above equation, the two contribution coefficients for thermal-expansion effect a_E and thermal-optical effect a_O for the MKR temperature probe can be determined to be 3.879×10^3 and 1.317×10^4, respectively. The impact from the thermal-optical effect is ~3.4 folds higher than that of the thermal-expansion effect for this temperature probe. The high temperature sensitivity, miniature and stable structure of the proposed temperature probe will enable its promising candidate for precisely sensing the temperature fluctuation for some special biochemical reactions and industry control process. Furthermore, the sensing performance seriously depends on the morphology parameter of MKR, the sensitive materials and packaged structures.

Conclusions

In summary, a PDMS-packaged MKR temperature sensor was demonstrated with a high sensitivity and good stability. The >9 folds higher sensitivity of 1.67 nm/°C was obtained experimentally comparing with the sensitivity of 183 pm/°C for the bare MKR. The MKR structure was sandwich-packaged between two glass slides, in which the PDMS sol was filled. Its thickness was precisely controlled as 0.6 mm by two Teflon tubes being inserted between the slides. The contributions for the thermal-expansion effect and thermal-optical effect have been analyzed and discussed as well.

Acknowledgments

This work was supported by Fundamental Research Funds for the Central Universities (N170405003 and N170407005), Liaoning Province Natural Science Foundation

(20180510015) and Liaoning Revitalization Talents Program (XLYC1807198).

References

[1] Liu D, Wu Q, Mei C, Yuan J, Xin X, Mallik AK, Wan S. Hollow core fiber based interferometer for high-temperature (1000°C) measurement. J Lightwave Technol. 2018; 36(9): 1583-1590.

[2] Liu YG, Liu X, Zhang T, Zhang W. Integrated FPI-FBG composite all-fiber sensor for simultaneous measurement of liquid refractive index and temperature. Opt Laser Eng. 2018; 111: 167-171.

[3] Trung TQ, Ramasundaram S, Hwang BU, Lee NE. An all-elastomeric transparent and stretchable temperature sensor for body-attachable wearable electronics. Adv Mater. 2015; 28(3): 502-509.

[4] Liu Q, Li S, Chen H, Fan Z, Li J. Photonic crystal fiber temperature sensor based on coupling between liquid-core mode and defect mode. IEEE Photon J. 2015; 7(2): 1-9.

[5] Jia Z, Pu S, Rao J, Zhao Y, Li Y, Yao T. Temperature self-compensative all-fiber magnetic field sensing structure based on no-core fiber cascaded with fiber Bragg gratings. Opt Laser Eng. 2019; 119: 26-29.

[6] Liu G, Han M, Hou W. High-resolution and fast-response fiber-optic temperature sensor using silicon Fabry-Pérot cavity. Opt Express. 2015; 23(6): 7237-7247.

[7] Shao LY, Luo Y, Zhang Z, Zou X, Luo B, Pan W, Yan L. Sensitivity-enhanced temperature sensor with cascaded fiber optic Sagnac interferometers based on Vernier-effect. Opt Commun. 2015; 336: 73-76.

[8] Wang Q, Kong L, Dang Y, Xia F, Zhang Y, Zhao Y, Li J. High sensitivity refractive index sensor based on splicing points tapered SMF-PCF-SMF structure Mach-Zehnder mode interferometer. Sensor Actuat B-Chem. 2016; 225: 213-220.

[9] Woyessa G, Fasano A, Markos C, Stefani A, Rasmussen HK, Bang O. Zeonex microstructured polymer optical fiber: fabrication friendly fibers for high temperature and humidity insensitive Bragg grating sensing. Opt Mater Express. 2017; 7(1): 286-295.

[10] Nguyen LV, Warren-Smith SC, Ebendorff-Heidepriem H, Monro TM. Interferometric high temperature sensor using suspended-core optical fibers. Opt Express. 2016; 24(8): 8967-8977.

[11] Van Newkirk A, Antonio-Lopez E, Salceda-Delgado G, Amezcua-Correa R, Schülzgen A. Optimization of multicore fiber for high-temperature sensing. Optics Letters. 2014; 39(16): 4812-4815.

[12] Hnatovsky C, Grobnic D, Mihailov SJ. Birefringent π-phase-shifted fiber Bragg gratings for sensing at 1000° C fabricated using an infrared femtosecond laser and a phase mask. Journal of Lightwave Technology. 2018; 36(23): 5697-5703.

[13] Kim HT, Yu M. Cascaded ring resonator-based temperature sensor with simultaneously enhanced sensitivity and range. Opt Express. 2016; 24(9): 9501-9510.

[14] Li J, Fan P, Tian Z, Sun LP, Guan BO. Potential for simultaneous measurement of magnetic field and temperature utilizing fiber taper modal interferometer and magnetic fluid. IEEE Photon J. 2016; 8(6): 6805609.

[15] Militky J, KadulováM, Ciprian D, Hlubina P. Fiber optic temperature sensing with enhanced sensitivity based on spectral interferometry. Opt Fiber Technol. 2017; 33: 45-50.

[16] Miao YP, He Y, Ma XX, Zhang H, Song BB, Yang XP, Xue LF, Liu B, Yao JQ. Low-temperature cross-sensitivity refractive index sensor based on single-mode fiber with periodically modulated taper. IEEE Sensor J. 2016; 16(8): 2442-2446.

[17] Fan R, Mu ZZ, Li J. Miniature temperature sensor based on polymer-packaged silica microfiber resonator. J Phys Chem Sol. 2019; 129: 307-311.

[18] Chen GW, Zhang ZJ, Wang XL, Li HG, Jiang MJ, Guan HY, Qiu WT, Lu HH, Dong JL, Zhu WG, Yu JH, Zhong YC, Luo YH, Zhang J, Chen Z. Highly sensitive all-optical control of light in WS2 coated microfiber knot resonator. Opt Express. 2018; 26(21): 27650-27658.

[19] Dass S, Jha R. Square knot resonator-based compact bending sensor. IEEE Photon Technol Lett. 2018; 30(18): 1649-1652.

[20] Wu Y, Rao YJ, Chen YH, Gong Y. Miniature fiber-optic temperature sensors based on silica/polymer microfiber knot resonators. Opt Express. 2018; 17(20): 18142-18147.

[21] Yang H, Wang S, Wang X, Wang J, Liao Y. Temperature sensing in seawater based on microfiber knot resonator. Sensors. 2014; 14(10): 18515-18525.

[22] Shin JC, Yoon MS, Han YG. Relative humidity sensor based on an optical microfiber knot resonator with a polyvinyl alcohol overlay. J Lightwave Technol. 2016; 34: 4511-4515.

[23] Pu SL, Mao LM, Yao TJ, Gu JF, Lahoubi M, Zeng XL. Microfiber coupling structures for magnetic field sensing with enhanced sensitivity. IEEE Sensor J. 2017; 99(18): 5857-5861.

[24] Le ADD, Han YG. Relative humidity sensor based on a few-mode microfiber knot resonator by mitigating the group index difference of a few-mode microfiber. J Lightwave Technol. 2018; 36(4): 904-909.

[25] Wang MQ, Li D, Wang RD, Zhu J, Ren Z. PDMS-assisted graphene microfiber ring resonator for temperature sensor. Opt Quantum Electron. 2018; 50: 132-134.

[26] Lim K.S, Aryanfar I, Chong W.Y, Cheong Y.K, S Harun.W, Ahmad H. Integrated microfibre device for refractive index and temperature sensing. Sensors. 2012; 12(9): 11782-11789.

[27] Yang H, Wang S, Mao K, Li G, Wang J. Numerical calculation of seawater temperature sensing based on polydimethylsiloxane-coated microfiber knot resonator. Opt Photon J. v2014; 4: 91-97.

[28] Tada H, Kumpel AE, Lathrop RE, Slanina JB, Nieva P, Zavracky P, Miaoulis IN, Wong PY. Thermal expansion coefficient of polycrystalline silicon and silicon dioxide thin films at high temperatures. J Appl Phys. 2000; 87(9): 4189-4193.

[29] Bowden N, Huck WT, Paul KE, Whitesides GM. The controlled formation of ordered, sinusoidal structures by plasma oxidation of an elastomeric polymer. Appl Phys Lett. 1999; 75(17): 2557-2559.

[30] He L, Xiao YF, Zhu J, Ozdemir SK, Yang L. Oscillatory thermal dynamics in high-Q PDMS-coated silica toroidal microresonators. Opt Express. 2009; 17(12): 9571-9581.